

LA-UR- 01-3339

*Approved for public release;  
distribution is unlimited.*

*Title:* Embedded Electromagnetic Gauge Measurements and Modeling of Shock Initiation in the TATB based Explosives PBX 9502 and LX-17

*Author(s):* R. L. Gustavsen, S. A. Sheffield, and R. R. Alcon  
Los Alamos National Laboratory, Los Alamos, NM

J.W. Forbes, C.M. Tarver, and F. Garcia  
Lawrence Livermore National Laboratory, Livermore, CA

*Submitted to:* Shock01 meeting of the American Physical Society, June 24-29  
2001, Atlanta, GA

# Los Alamos

NATIONAL LABORATORY

Los Alamos National Laboratory, an affirmative action/equal opportunity employer, is operated by the University of California for the U.S. Department of Energy under contract W-7405-ENG-36. By acceptance of this article, the publisher recognizes that the U.S. Government retains a nonexclusive, royalty-free license to publish or reproduce the published form of this contribution, or to allow others to do so, for U.S. Government purposes. Los Alamos National Laboratory requests that the publisher identify this article as work performed under the auspices of the U.S. Department of Energy. Los Alamos National Laboratory strongly supports academic freedom and a researcher's right to publish; as an institution, however, the Laboratory does not endorse the viewpoint of a publication or guarantee its technical correctness.

# EMBEDDED ELECTROMAGNETIC GAUGE MEASUREMENTS AND MODELING OF SHOCK INITIATION IN THE TATB BASED EXPLOSIVES LX-17 AND PBX 9502<sup>†</sup>

R. L. Gustavsen, S. A. Sheffield, R. R. Alcon<sup>1</sup> J.W. Forbes, C.M. Tarver, and F. Garcia<sup>2</sup>

<sup>1</sup>*Los Alamos National Laboratory, Los Alamos, NM 87545*

<sup>2</sup>*Lawrence Livermore National Laboratory, Livermore, CA 94550*

We have completed a series of shock initiation experiments on PBX 9502 (95 weight % dry aminated TATB explosive, 5 weight % Kel-F 800 binder) and LX-17 (92.0% wet aminated TATB, 7.5 % Kel-F 800). These experiments were performed on the gas/gas two stage gun at Los Alamos. Samples were prepared with ten or eleven embedded electromagnetic particle velocity gauges to measure the evolution of the wave leading up to a detonation. Additionally, one to three shock tracker gauges were used to track the position of the shock front with time and determine the point where detonation was achieved. Wave profiles indicate little delay between formation of hot-spots in the shock front and release of hot-spot energy. In other words, a great deal of the buildup occurs in the shock front, rather than behind it. Run distances and times to detonation as a function of initial pressure are consistent with published data. The Ignition and Growth model with published parameters for LX-17 replicate the data very well.

## INTRODUCTION

The TATB based explosives LX-17 and PBX 9502 are among the most thoroughly studied high explosives in current use. References 1-6 provide examples of work on these explosives, which we will refer to throughout this paper. The reasons for interest in these explosives are their insensitivity to initiation by shock and heat, their high power, and their manufacturability. By manufacturability, we mean that uniform density pressings can be made and from these, parts are easily and safely machined

One of the finest methods for measuring the shock initiation of detonation in explosives is the embedded multiple electromagnetic particle velocity gauge method developed and used at Los Alamos.<sup>7</sup> Until recently, this method could not be applied to these insensitive TATB based explosives. The reason for this is that very high shock pressures are needed to initiate these explosives. These pressures can be achieved with  $\sim 2$  km/s projectile velocities achievable with powder guns and high impedance metallic impactors such as copper or stainless steel. However, electromagnetic particle velocity gauge measurements cannot be made using metallic (con-

ducting) impactors or projectiles because of the eddy currents produced as the metal moves through the magnetic field.

About 5 years ago, we started doing shots on the Los Alamos 50 mm bore gas driven two-stage gun. This gun is capable of the 2 – 3 km/s projectile velocities needed to initiate TATB based explosives using plastic impactors. Unfortunately, being the only gun of its kind, it has had a lengthy shakedown period. We have encountered projectiles which disintegrated when launched, huge impact tilts, gouged barrels, and projectile velocity measuring systems that refused to work. Fortunately, this is now behind us. Hereafter, we present our progress on making embedded magnetic particle velocity gauge measurements in these insensitive explosives. Throughout, we will try to show that our work is in accord with, and complementary to, the fine previous studies.

## EXPERIMENTAL DETAILS

The overall configuration for the initiation experiments is shown in Figure 1. This is the same configuration described in great detail in Ref. 7. A

<sup>†</sup> Work performed under the auspices of the U.S. Dept. of Energy.

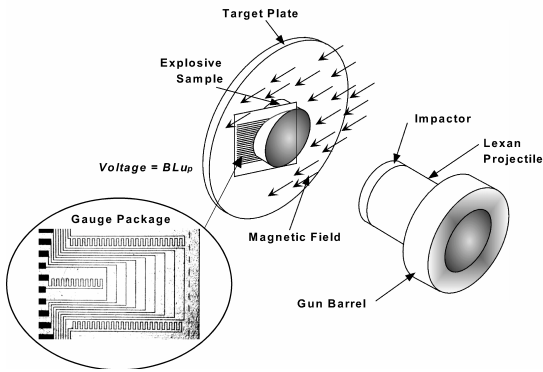


**FIGURE 1.** Experimental setup. Explosive sample installed in gun target chamber and magnetic field.

Lexan projectile is faced with an impactor disk made of Kel-F, a high-density plastic, and coincidentally, the binder material for the explosives studied. Because of our problem with projectiles disintegrating when launched, we have till now been reluctant to use impactors made of anything but plastic.

In all but one of the experiments, the projectile velocity was measured using optical methods. We must confess, however, that the optical method changed from one experiment to the next as “improvements” were made. Nevertheless, all the methods we used gave standard errors in the velocity of  $< 10$  m/s.

When the impactor strikes the explosive sample, a planar shock wave is generated which begins the initiation process. The stress of the initial shock is determined using the impact velocity, the Hugoniot of the Kel-F impactor,<sup>8</sup> the Hugoniot of the explosive,<sup>9</sup> and standard impedance matching techniques.

Electromagnetic particle velocity gauges are embedded in the explosive sample at ten or eleven different depths. These vary from the impact surface to about 11 mm into the sample. These, of course, produce voltages proportional to the local mass (particle) velocity at the Lagrangian position of the gauge. Three “shock trackers” also allow construction of distance - time ( $x-t$ ) plots of the position of the shock front with time as it moves through the sample. These  $x-t$  trajectories are used to determine the position and time where detonation is achieved.

## EXPERIMENTAL RESULTS

Wave profiles of particle velocity vs. time and  $x-t$  plots of the shock trajectories were successfully obtained for eight experiments on PBX 9502 and

three experiments on LX-17. In addition, there were many additional experiments that failed for one reason or another. Impact stresses of 10.8 to 15.4 Gpa were created with projectile velocities of 2.4 to 3 km/s. This produced run distances of 4.4 to over 14 mm.

Figure 2 shows wave-profiles from shot 2S-47 where LX-17 was impacted with a Kel-F impactor at a velocity of  $2.951 \pm 0.004$  km/s producing an input of 14.96 GPa. The data quality is seen to be exceptional in this figure. Surprisingly, this quality was typical for experiments that worked. Experiments that didn’t work failed in an unmistakable fashion. Nine good wave profiles from gauges located at depths of 0.0 through 6.7 mm were recorded. The first profile is from a gauge on the front of the sample and the remaining 8 from embedded gauges. The input particle velocity is 1.45 km/s and this grows to a full detonation well before the wave reaches the last gauge.

All wave profiles other than the first show that the amplitude of the wave at the shock front is increasing as the wave travels into the sample. This is observed in all heterogeneous explosives. Additionally, there is a small hump behind the shock front. This is consistent with some delay between the shock passing through un-shocked material and the release of energy.

Additionally, as observed by Wackerle, Stacy and Seitz,<sup>6</sup> the slope of the particle velocity immediately behind the shock front is positive. This per-

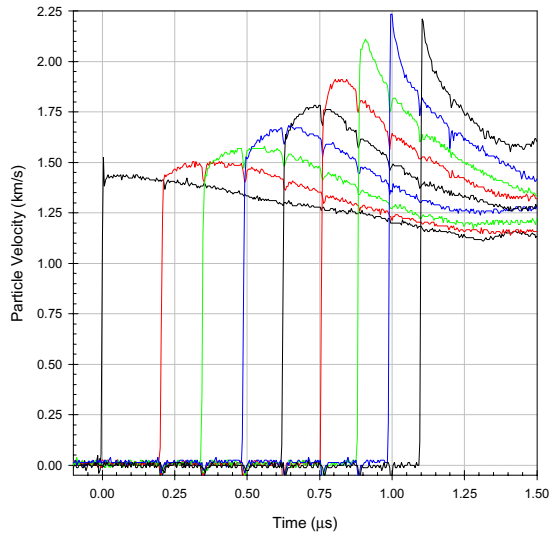


**FIGURE 2.** Particle velocity wave profiles from shot 2S-47 on LX-17. The input is 14.96 GPa and was created by impacting Kel-F on the LX-17 at 2.951 km/s.

sists and is observable up until detonation is achieved, and only then can it not be resolved. This is indicative variously of a slow initial reaction or an induction time before reaction begins. The models of Tarver and also of Pier Tang account for this using a weak or slow initial reaction rate.

When one accounts for the  $\sim 40$  ns time response of the embedded gauges, the detonation wave profiles are consistent with those observed in Refs. 4 and 6 using Fabry-Perot Velocimetry. That is, after the initial shock, the time to go from  $\sim 2.2$  km/s to 1.5 km/s is roughly the same for both types of experiments. Additionally, in Refs. 4 and 5, the time to drop from the spike at  $\sim 2.65$  km/s to  $\sim 2.2$  km/s, where our records begin, is very short  $\sim 40 - 50$  ns which is roughly the time response of our gauges.

The  $x$ - $t$  plot showing the position of the shock front with time is shown in Figure 3. This again is for shot 2S-47 in LX-17. Points shown are from all three shock tracker gauges and the particle velocity gauges. The slope of the line through the last few data points indicates the detonation velocity.

From plots such as those shown in Figure 3, there are a number of ways to determine the run distance and time to detonation. Because the approach to detonation in these TATB based explosives is so gradual, we have found it useful to use the point where the data closely approach the detonation line as the transition point. Even so, it is often helpful to have the guidance of corresponding

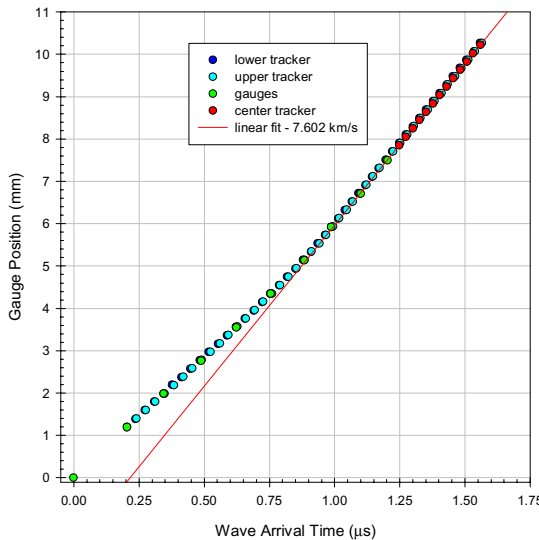


FIGURE 3.  $x$ - $t$  plot obtained from shock arrival at shock tracker elements and particle velocity gauge elements. The shot is #2S-47 on LX-17.

wave profiles such as those in Figure 2.

Figure 4 shows “Pop – Plots” of distance to detonation as a function of the initial shock pressure. Historic work for PBX 9502 (Ref. 2) and LX-17 (Refs. 1,3,5) is shown as well as data from the present study. Note first that PBX 9502 is slightly more sensitive than LX-17. This is due to; 1) slightly more explosive and less binder in the PBX 9502; 2) For the case of  $1.900 \text{ g/cm}^3$  LX-17, PBX 9502 and LX-17 have nearly identical void content of  $\sim 2.6 - 2.7\%$ . The reason for the decreased sensitivity in LX-17 in the work of Dallman and Wackerle is that the explosive they used had a lower void content  $\sim 2.0\%$  (density  $1.913 \text{ g/cm}^3$ ).

PBX 9502 data shown in the Pop – Plot of Figure 4 is from three powder lots. Dick et. al.<sup>2</sup> used explosive pressed from “Virgin” PBX 9502 molding powder. Our work used two different lots of “Recycled” PBX 9502 molding powder. Recycled molding powder is made from 50% Virgin molding powder and 50% ground up machining scraps. All sets of data lie on the same curve. The Pop – Plot for PBX 9502 is thus,

$$\log(X) = 4.26 \pm 0.09 - (3.06 \pm 0.08) \log(P). \quad (1)$$

This work and Jackson et. al.<sup>1</sup> used LX-17 pressed to  $1.900 \text{ g/cm}^3$  from two different molding powder lots. The Pop – Plots for this density of LX – 17 is

$$\log(X) = 4.53 \pm 0.12 + (3.22 \pm 0.10) \log(P). \quad (2)$$

Dallman and Wackerle<sup>7</sup> used LX-17 pressed at Pantex to a density of  $1.913 \text{ g/cm}^3$ . The Pop – Plot for this material is

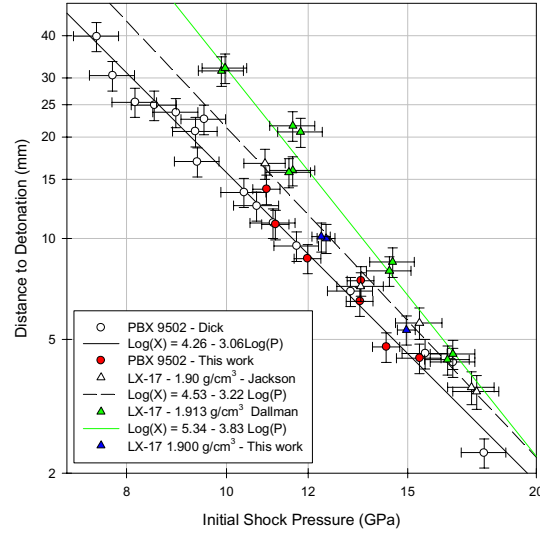


FIGURE 5. Pop – plots for TATB based explosives. Names of first authors identify data sets.

$$\log(X) = 5.34 \pm 0.26 - (3.83 \pm 0.23) \log(P). \quad (3)$$

## NUMERICAL MODELING

We used the Ignition and Growth “Reactive Burn” model to simulate these experiments. As with all reactive burn models, equations of state are required for the unreacted explosive and for the reaction products. We used the JWL model for these equations of state

$$P = A \exp(-R_1 V / V_0) + B \exp(-R_2 V / V_0) + \omega C_V T V_0 / V \quad (4)$$

Table 1 gives EOS parameters for LX-17 and PBX 9502 products and unreacted explosive. Note that aside from the initial volume, both explosives have identical Equations of State.

**Table 1.** EOS Parameters for LX-17 and PBX 9502

Parameter Eq.(4)	Unreacted EOS (PBX 9502)	Product EOS
<b>A</b> (Mbar)	632.07	13.454
<b>B</b> (Mbar)	-0.04472	0.6727
<b>R</b> <sub>1</sub>	11.3	6.2
<b>R</b> <sub>2</sub>	1.13	2.2
<b>ω</b>	0.8938	0.5
<b>C<sub>V</sub></b> *10 <sup>-5</sup> (Mbar/K)	2.487	1.0
<b>V<sub>0</sub></b> (cm <sup>3</sup> /g)	0.525 (0.531)	
<b>E<sub>0</sub></b> (Mbar)		0.069
<b>D</b> (cm/μs)		0.7596
<b>P<sub>CJ</sub></b> (Mbar)		0.2714

The Ignition and Growth reactive burn model was used, where  $\lambda$  is the fraction reacted is

$$d\lambda/dt = I_0(1-\lambda)^{2/3}(\rho/\rho_0 - 1 - a) + G_1(1-\lambda)^{2/3}\lambda^{0.11}P^1 + G_2(1-\lambda)^{1/3}\lambda^1P^2 \quad (5)$$

Table 2 lists Parameters used for the reaction modeling. Note again that most parameters were the same for both explosives. The lower value of  $a$  for PBX 9502 indicates that this explosive starts reacting at a slightly lower pressure or compression. There was not room in this paper to include comparison between the measured and calculated wave profiles, but these parameters have been found to model all of the available data very well. A more complete paper including all the data and these comparisons will be published later.

**Table 2.** Ignition and Growth reactive burn parameters.

Parameter Eq. (5)	LX-17	PBX 9502
<b>I<sub>0</sub></b> (1/μs)	<b>4.4(10<sup>5</sup>)</b>	<b>4.4(10<sup>5</sup>)</b>
<b>G<sub>1</sub></b> (Mbar <sup>-1</sup> μs <sup>-1</sup> )	<b>0.6</b>	<b>0.6</b>
<b>G<sub>2</sub></b> (Mbar <sup>-2</sup> μs <sup>-1</sup> )	<b>400</b>	<b>400</b>
<b>a</b>	<b>0.22</b>	<b>0.214</b>
<b>X</b>	<b>7.0</b>	<b>7.0</b>
<b>Z</b>	<b>3.0</b>	<b>3.0</b>

## ACKNOWLEDGEMENTS

Robert Medina operated the gas gun for all of the experiments presented here.

## REFERENCES

1. R.K. Jackson, L.G. Green, R.H. Barlett, W.W. Hofer, P.E. Kramer, R.S. Lee, E.J. Nidick, Jr., L.L. Shaw, and R.C. Weingart in *Proceedings of the Sixth Symposium (International) on Detonation*, Office of Naval Research, Report ACR-221, p. 755, 1976
2. Jerry J. Dick, C.A. Forest, J.B. Ramsay, and W.L. Seitz,, *J. Appl. Phys.*, **63**, 4881, (1988)
3. K. Bahl, G. Bloom, L. Erickson, R. Lee, C. Tarver, W. Von Holle, and R. Weingart in *Proceedings of the Eighth Symposium (International) on Detonation*, Office of Naval Research, Report NSWC MP 86-194, p. 1045, 1986
4. W.L. Seitz, H.L. Stacy, Ray Engelke, P.K. Tang, and Jerry Wackerle in *Proceedings of the Ninth Symposium (International) on Detonation*, Office of Naval Research, Report OCNR 113291-7, p. 657, 1989
5. J.C. Dallman and Jerry Wackerle in *Proceedings of the Tenth Symposium (International) on Detonation*, Office of Naval Research, Report ONR 33395-12, p. 130, 1995
6. Jerry Wackerle, H.L. Stacy, and W.L. Seitz in *Proceedings of the Tenth Symposium (International) on Detonation*, Office of Naval Research, Report ONR 33395-12, p. 468, 1995
7. S.A. Sheffield, R.L. Gustavsen and R.R. Alcon, in *Shock Compression of Condensed Matter – 1999*, American Institute of Physics (AIP) Conference Proceedings 505 (1999), p. 1043.
8.  $\rho_0 = 2.14 \text{ g/cm}^3$ ,  $U_s = 1.99 + 1.76u_p \text{ km/s}$   
S.A. Sheffield and R.R. Alcon, in *Shock Compression of Condensed Matter – 1991*, S.C. Schmidt, R.D. Dick, J.W. Forbes, D.G. Tasker (editors), Elsevier Science Publishers (1992), p. 909.
9.  $U_s = 1.90 + 3.00u_p : u_p \leq 0.82$   
 $U_s = 2.90 + 1.78u_p : u_p \geq 0.82$   
C.A Forest, unpublished (1995). This Hugoniot for PBX 9502 is based primarily on the data of Ref. 2.